Available online at www.sciencedirect.com
SCIENCE DIRECT
Journal of Sound and Vibration 296 (2006) 353–367
JOURNAL OF SOUND AND VIBRATION
www.elsevier.com/locate/jsvi

Free vibration of rotating ring stiffened cylindrical shells with non-uniform stiffener distribution

A.A. Jafari[a,*], M. Bagheri[b]

[a]Department of Mechanical Engineering, K. N. Toosi University of Technology, P.O. Box 16765-3381, Tehran, Iran
[b]Faculty of Aerospace Engineering, Shahid Sattari Air University, Tehran, Iran

Received 24 May 2004; received in revised form 9 January 2006; accepted 7 March 2006
Available online 6 May 2006

Abstract

In this research, the free vibration analysis of simply supported rotating cylindrical shells with circumferential stiffeners, i.e. rings with non-uniform stiffeners eccentricity and non-uniform stiffeners spacing distribution is investigated. Ritz method is applied while stiffeners are treated as discrete elements. In strain energy formulation, by adopting Sander's theorem, stretching and bending characteristics of shells are considered. Also stretching, bending and wrapping effects of stiffeners are investigated. The translational inertia in three directions for shell and stiffeners, and rotary inertia for stiffeners are considered. The effects of initial hoop tension, centrifugal and Coriolis forces due to the rotation of shell are studied. The polynomial functions are used for Ritz functions. Natural frequency results for rings with uniform spacing and constant eccentricity have been compared with analytical and experimental results of other researchers, which showed good agreement. Fortunately, the agreements of the presented analytical results with the experimental values are better than the analytical values. At constant total mass of stiffeners, the effects of non-uniform eccentricity distribution and non-uniform rings spacing distribution (separately and simultaneously) on natural frequencies are investigated. Moreover, the influence of rotating speed on natural frequencies for the so-called non-uniform stiffeners distribution is studied.

1. Introduction

Ring stiffened cylindrical shells are applied in many structures such as pressure vessels, submarine hulls, aircraft, launch vehicles and offshore drilling rigs. The knowledge of these structures characteristics is necessary to determine their structural integrity and fatigue life. The natural frequencies of vibrations are of special interest to aircraft and launch vehicle designers because of increasing use of sensitive electronic instrumentation and on-board computers and gyroscopes, which require vibration isolation from the main structure.

In the considerable literature on this subject, there are two main types of analysis, depending upon whether the stiffening rings are treated by averaging their properties over the surface of the shell or by considering them as discrete elements. When ring stiffeners of equal strength are closely and evenly spaced, the stiffened

*Corresponding author. Tel.: +98 21 77343300; fax: +98 21 77334338.
E-mail address: bagheri@alborz.kntu.ac.ir (A.A. Jafari).

0022-460X/$ - see front matter © 2006 Elsevier Ltd. All rights reserved.
doi:10.1016/j.jsv.2006.03.001

shell can be modeled as an equivalent orthotropic shell. This is also called smearing method. However, as the stiffener spacing increases or the wavelength of vibration becomes smaller than the stiffener spacing, the determination of dynamic characteristics of stiffened shell is not accurate. Thus, for a more general model, the ring stiffeners have to be treated as discrete elements. When modeled in this respect, it is advantageous to use non-uniform eccentricity, unequally spaced and different materials for ring stiffeners.

The free vibration of stiffened cylindrical shells has been investigated since 1950s by a number of researchers. Hopmann [1] investigated the free vibration of orthogonally stiffened cylindrical shells with simply supported ends, analytically and experimentally. In this study smearing method for stiffeners was used in the analytical investigation. Mikulas and McElman [2] investigated the free vibration of eccentrically stiffened simply supported cylindrical shells by averaging the stiffeners properties over the surface of the shells and found that the eccentricity could have significant effects on natural frequencies. Egle and Sewall [3] extended this study with stiffeners treated as discrete elements. The effects of in-plane and rotary inertia on the natural frequencies of eccentrically stiffened shells were examined by Parthan and Johns [4]. A theoretical and experimental investigation of the vibration of axially loaded stiffened cylindrical shells was provided by Rosen and Singer [5] using Donell and Flugge theories. Mustafa and Ali [6] presented an energy method for free vibration analysis of stiffened cylindrical shells. The analysis took into account the flexure and extension of the shell and the flexure, extension and torsion of the stiffeners. Lim and Liew [7] presented a flexural free vibration analysis of shallow cylindrical shells for different boundary conditions combinations. In this study, Ritz method was used which the in-plane and transverse displacements assumed in the form of orthogonal polynomials. Liew and Lim [8,9] developed a continuum Ritz model for twisted plate vibration and variable thickness shallow cylindrical shells vibration, using aforementioned polynomials functions for in-plane and transverse displacements. Swaddiwudhipong et al. [10] presented the free vibrations of cylindrical shells with rigid intermediate supports utilizing Ritz method. A special polynomial unified set of Ritz function was used to span the displacement fields of various types and combinations of end boundary conditions. Wang et al. [11] extended the Ritz method for solving the free vibration problem of cylindrical shells with varying ring stiffener distributions.

The behavior of rotating cylindrical shells was first investigated by Bryan [12] and it was in this work that traveling modes were first elucidated. The effects of Coriolis and centrifugal forces in rotating shell structures have been examined by DiTaranto and Lessen [13] and Huang and Soedel [14]. Zhao et al. [15] presented the free vibration analysis of simply supported rotating cross-ply laminated cylindrical shells with axial and circumferential stiffeners, using an energy approach. The effects of these stiffeners were evaluated via two methods: stiffeners treated as discrete elements; and the properties of the stiffeners were averaged over the shell surface by smearing method. Liew et al. [16] proposed a meshfree approach—the harmonic reproducing kernel particle method for the free vibration analysis of rotating cylindrical shells. The effects of centrifugal and Coriolis forces as well as the initial hoop tension due to rotation are all taken into account.

This paper extends the method used by Lim and Liew [7] and Wang et al. [11] for free vibration analysis of rotating ring stiffened cylindrical shells with non-uniform stiffeners distribution. They investigated the effects of non-uniform eccentricity distribution and non-uniform rings spacing distribution separately, on natural frequencies of non-rotating ring stiffened shell for a few cases of non-uniformity. However, the present research contributes the above effects both separately and simultaneously for a wide range of non-uniformity of rotating ring stiffened cylindrical shells. At constant total mass of stiffeners, the effects of non-uniformity and rotating speed of either internally or externally ring stiffened cylindrical shell on natural frequencies are investigated. More attention is paid to fundamental and beam mode frequencies. Furthermore, bifurcation of natural frequencies due to rotation speed and Coriolis acceleration is investigated. In the case of uniform stiffeners eccentricity and equal stiffeners spacing, present results have been compared with experimental and analytical results of other researchers.

Although, the free vibration problem of stiffened shell can be solved by using popular commercial software, but the present analytical method investigated the effects of non-uniform stiffeners eccentricity distribution and non-uniform stiffeners spacing distribution on dynamic characteristics of rotating stiffened cylindrical shells, simultaneously. Moreover, the present method is suitable for optimization problem of non-uniformly stiffened cylindrical shells with various boundary conditions combinations.

2. Theoretical formulation

The cylindrical shell as shown in Fig. 1 is considered to be thin with a uniform thickness h, radius R, length L, mass density ρ, modulus of elasticity E, Poisson's ratio v shear modulus $G = E/2(1+v)$ and rotation speed ϖ. The shell is circumferentially stiffened by N number of rings, which may be placed internally or externally. The κth ring stiffener has a rectangular cross section of constant width br_κ and depth dr_κ, and is located at the distance $a_\kappa L$ from one end of the shell. The rings spacing and rings depth may be varied along the length of the shell. The ring-stiffeners may be constructed from different materials from one another and also from the parent shell material. The κth stiffener properties are defined as mass density ρr_κ, modulus of elasticity Er_κ, Poisson's ratio vr_κ and shear modulus Gr_κ.

2.1. Shell energy

Based on Sander's [17] thin shell theory, the strain energy of stretching and bending of the aforementioned cylindrical shell without stiffeners is expressed as:

$$U_\varepsilon = \int_0^L \int_0^{2\pi} \left\{ \frac{Eh}{2(1-v^2)} \left[\left(\frac{\partial u}{\partial x}\right)^2 + \frac{1}{R^2}\left(\frac{\partial v}{\partial \theta} - w\right)^2 + \frac{2v}{R}\left(\frac{\partial u}{\partial x}\right)\left(\frac{\partial v}{\partial \theta} - w\right) + \frac{1-v}{2}\left(\frac{\partial v}{\partial x} + \frac{1}{R}\frac{\partial u}{\partial \theta}\right)^2 \right] + \frac{Eh^3}{24(1-v^2)} \times \left[\left(\frac{\partial^2 w}{\partial x^2}\right)^2 + \frac{1}{R^4}\left(\frac{\partial^2 w}{\partial \theta^2} + \frac{\partial v}{\partial \theta}\right)^2 + \frac{2v}{R^2}\left(\frac{\partial^2 w}{\partial x^2}\right)\left(\frac{\partial^2 w}{\partial \theta^2} + \frac{\partial v}{\partial \theta}\right) + \frac{2(1-v)}{R^2}\left(\frac{\partial^2 w}{\partial x\,\partial \theta} + \frac{3}{4}\frac{\partial v}{\partial x} - \frac{1}{4R}\frac{\partial u}{\partial \theta}\right)^2 \right] \right\} R\,\mathrm{d}\theta\,\mathrm{d}x, \tag{1}$$

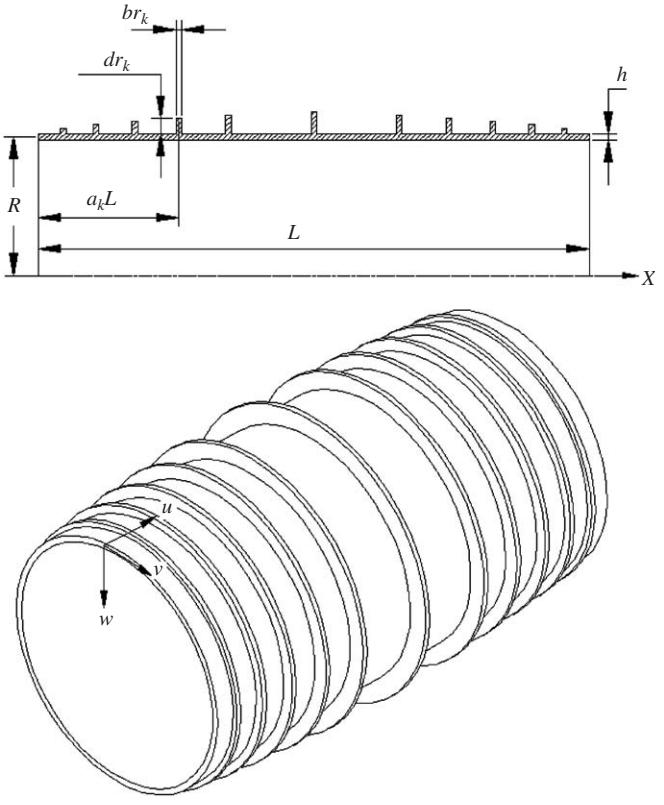

Fig. 1. A ring stiffened cylindrical shell with non-uniform stiffeners distribution.

where u, v, w are displacements in the longitudinal, tangential and radial directions, respectively, x, θ are longitudinal and circumferential coordinates respectively, as shown in Fig. 1.

The initial hoop tension due to the centrifugal force is defined as

$$N_\theta = \rho h R^2 \varpi^2 \tag{2}$$

and the strain energy of the shell due to the hoop tension is:

$$U_h = \frac{1}{2}\int_0^L \int_0^{2\pi} N_\theta \left\{ \frac{1}{R^2}\left(\frac{\partial u}{\partial \theta}\right)^2 + \frac{1}{R^2}\left(\frac{\partial v}{\partial \theta} - w\right)^2 + \frac{1}{R^2}\left(\frac{\partial w}{\partial \theta} + v\right)^2 \right\} R \, \mathrm{d}\theta \, \mathrm{d}x. \tag{3}$$

Neglecting the effect of rotary inertia since the shell under consideration is thin; the kinetic energy of a rotating cylindrical shell without stiffeners is expressed as

$$T = \frac{1}{2}\rho h \int_0^L \int_0^{2\pi} \left\{ \left(\frac{\partial u}{\partial t}\right)^2 + \left(\frac{\partial v}{\partial t}\right)^2 + \left(\frac{\partial w}{\partial t}\right)^2 + 2\varpi(v\dot{w} - w\dot{v}) + \varpi^2(v^2 + w^2) \right\} R \, \mathrm{d}\theta \, \mathrm{d}x. \tag{4}$$

2.2. Ring stiffener energy

In this analysis, geometric characteristics and materials of the rings may be different from one another. Also rings spacing and their eccentricity can have non-uniform distributions.

The strain energy of the κth ring stiffener with the effects of stretching, biaxial bending and wrapping is given by

$$\begin{aligned} Ur_\kappa = \int_0^{2\pi} \Bigg\{ & \frac{Er_\kappa Izr_\kappa}{2} \frac{1}{R + er_\kappa} \left(\frac{\partial wr_\kappa}{\partial x} + \frac{1}{R + er_\kappa} \frac{\partial^2 ur_\kappa}{\partial \theta^2} \right)^2 + \frac{Er_\kappa Ixr_\kappa}{2} \frac{1}{(R + er_\kappa)^3} \left(wr_\kappa + \frac{1}{R + er_\kappa} \frac{\partial^2 wr_\kappa}{\partial \theta^2} \right)^2 \\ & + \frac{Er_\kappa Ar_\kappa}{2} \frac{1}{R + er_\kappa} \left(\frac{\partial vr_\kappa}{\partial \theta} - wr_\kappa \right) + \frac{Gr_\kappa Jr_\kappa}{2} \frac{1}{R + er_\kappa} \left(-\frac{\partial^2 wr_\kappa}{\partial x \, \partial \theta} + \frac{1}{R + er_\kappa} \frac{\partial ur_\kappa}{\partial \theta} \right)^2 \Bigg\} \mathrm{d}\theta, \end{aligned} \tag{5}$$

where Izr_κ, Ixr_κ are the second moments of areas of the κth ring stiffener about the x and z axes, Ar_κ is the cross-sectional area and Jr_κ is torsional rigidity, which are determined by

$$Izr_\kappa = \frac{br_\kappa^3 dr_\kappa}{12}, \quad Ixr_\kappa = \frac{br_\kappa dr_\kappa^3}{12}, \quad Ar_\kappa = br_\kappa dr_\kappa, \quad Jr_\kappa = \frac{1}{3}\left[1 - \frac{192 br_\kappa}{\pi^5 dr_\kappa} \sum_{n=1,3,5,\ldots}^{\infty} \frac{1}{n^5} \tanh \frac{n\pi dr_\kappa}{2br_\kappa} \right] br_\kappa^3 dr_\kappa \tag{6}$$

and er_κ is the eccentricity of the κth ring stiffener as follows:

$$er_\kappa = \pm \frac{h + dr_\kappa}{2}, \tag{7}$$

where the sign (+) represents external stiffening and sign (−) is used for internal stiffening.

The strain energy of the κth ring stiffener due to hoop tension is taken to be

$$\begin{aligned} Ur_{h\kappa} = \int_0^{2\pi} \frac{\overline{N}_\theta Ar_\kappa}{2} \Bigg\{ & \frac{1}{(R + er_\kappa)^2} \left(\frac{\partial ur_\kappa}{\partial \theta} \right)^2 + \frac{1}{(R + er_\kappa)^2} \left(\frac{\partial vr_\kappa}{\partial \theta} - wr_\kappa \right)^2 \\ & + \frac{1}{(R + er_\kappa)^2} \left(\frac{\partial wr_\kappa}{\partial \theta} + vr_\kappa \right)^2 \Bigg\} (R + er_\kappa) \, \mathrm{d}\theta, \end{aligned} \tag{8}$$

where initial hoop tension of the κth ring stiffener is defined as

$$\overline{N}_\theta = \rho r_\kappa (R + er_\kappa)^2 \varpi^2. \tag{9}$$

The kinetic energy of the κth rotating ring stiffener with the effects of triaxial translational inertia and rotary inertia about x and z axes is given by

$$Tr_\kappa = \frac{1}{2}\rho r_\kappa A r_\kappa \int_0^{2\pi} \left\{ \left[\left(\frac{\partial ur_\kappa}{\partial t}\right)^2 + \left(\frac{\partial vr_\kappa}{\partial t}\right)^2 + \left(\frac{\partial wr_\kappa}{\partial t}\right)^2 + 2\varpi(vr_\kappa \dot{w}r_\kappa - wr_\kappa \dot{v}r_\kappa) + \varpi^2(vr_\kappa^2 + wr_\kappa^2) \right] + (Ixr_\kappa(x) + Izr_\kappa(x)) \left(\frac{\partial^2 wr_\kappa}{\partial t\, \partial x}\right)^2 \right\} (R + er_\kappa)\, \mathrm{d}\theta. \tag{10}$$

From geometrical considerations, the relationships between the displacements $(ur_\kappa, vr_\kappa, wr_\kappa)$ of the κth stiffener and the displacements (u, v, w) of the shell at the position of the stiffener are given by:

$$ur_\kappa = u + er_\kappa \frac{\partial w}{\partial x}, \quad vr_\kappa = v\left(1 + \frac{er_\kappa}{R}\right) + \frac{er_\kappa}{R}\frac{\partial w}{\partial \theta}, \quad wr_\kappa = w. \tag{11}$$

Substituting Eqs. (6), (7), (11) into Eqs. (5), (8), (10), the ring stiffener energy can be written in the form of shell middle surface displacement.

Therefore, the energy functional of ring stiffened cylindrical shell can be written as

$$F = U_\varepsilon + U_h - T + \sum_{\kappa=1}^{N} (Ur_\kappa + Ur_{h\kappa} - Tr_\kappa). \tag{12}$$

The following functions are adopted to separate the spatial variable x, θ and the time variable t

$$u(x,\theta,t) = u(x)\sin(n\theta + \omega t), \quad v(x,\theta,t) = v(x)\cos(n\theta + \omega t), \quad w(x,\theta,t) = w(x)\sin(n\theta + \omega t), \tag{13}$$

where n is the number of circumferential waves and ω is circular frequency of vibration.

For generality and convenience, the following non-dimensional terms are defined:

$$\begin{aligned}
&\overline{u} = \frac{u}{h}, \quad \overline{v} = \frac{v}{h}, \quad \overline{w} = \frac{w}{R}, \quad \overline{x} = \frac{x}{L}, \quad \alpha = \frac{R}{L}, \quad \xi = \frac{h}{R}, \quad \overline{er}_\kappa = \frac{er_\kappa}{h},\\
&\overline{E}r_\kappa = \frac{Er_\kappa}{E}, \quad \overline{\rho}r_\kappa = \frac{\rho r_\kappa}{\rho}, \quad \overline{I}zr_\kappa = \frac{Izr_\kappa}{Rh^3}, \quad \overline{I}xr_\kappa = \frac{Ixr_\kappa}{Rh^3}, \quad \overline{A}r_\kappa = \frac{Ar_\kappa}{h^2},\\
&\overline{J}r_\kappa = \frac{Jr_\kappa}{Rh^3}, \quad \overline{F} = \frac{2(1-\nu^2)}{\pi hRLE}F, \quad \Omega^2 = \frac{(1-\nu^2)\rho R^2}{E}\omega^2, \quad \lambda^2 = \frac{(1-\nu^2)\rho R^2}{E}\varpi^2.
\end{aligned} \tag{14}$$

Using Eqs. (13) and (14), the non-dimensional total energy functional may be expressed as

$$\begin{aligned}
\overline{F} = \int_0^1 \Bigg\{ &\alpha^2\xi^2\left(\frac{\mathrm{d}\overline{u}}{\mathrm{d}\overline{x}}\right)^2 + (\xi n\overline{v} + \overline{w})^2 - 2\nu\alpha\xi\left(\frac{\mathrm{d}\overline{u}}{\mathrm{d}\overline{x}}\right)(\xi n\overline{v} + \overline{w}) + \frac{1-\nu}{2}\xi^2\left(\alpha\frac{\mathrm{d}\overline{v}}{\mathrm{d}\overline{x}} + n\overline{u}\right)^2\\
&+ \frac{\xi^2}{12}\left[\alpha^4\left(\frac{\mathrm{d}^2\overline{w}}{\mathrm{d}\overline{x}^2}\right)^2 + (n^2\overline{w} + n\xi\overline{v})^2 - 2\nu\alpha^2\left(\frac{\mathrm{d}^2\overline{w}}{\mathrm{d}\overline{x}^2}\right)(n^2\overline{w} + n\xi\overline{v}) + 2(1-\nu)\alpha^2\left(n\frac{\mathrm{d}\overline{w}}{\mathrm{d}\overline{x}} + \frac{3}{4}\xi\frac{\mathrm{d}\overline{v}}{\mathrm{d}\overline{x}} - \frac{n\xi}{4\alpha}\overline{u}\right)^2\right]\\
&+ \lambda^2\left[n^2\xi^2\overline{u}^2 + (n\xi\overline{v} + \overline{w})^2 + (n\overline{w} + \xi\overline{v})^2\right] - \Omega^2\left[\xi^2\overline{u}^2 + \xi^2\overline{v}^2 + \overline{w}^2\right]\\
&- 4\Omega\lambda\xi\overline{vw} - \lambda^2(\xi^2\overline{v}^2 + \overline{w}^2)\Bigg\}\,\mathrm{d}\overline{x} + \sum_{\kappa=1}^{N}\Bigg\{\frac{1-\nu^2}{(1+\xi\overline{er}_\kappa)^3}\overline{E}r_\kappa\alpha\xi^2\left[\overline{\mathscr{U}}r_{1\kappa} + \overline{\mathscr{U}}r_{2\kappa} + \overline{\mathscr{U}}r_{3\kappa} + \overline{\mathscr{U}}r_{4\kappa}\right]\\
&+ \overline{\rho}r_\kappa(1+\xi\overline{er}_\kappa)\alpha\xi\left(\lambda^2\left[\overline{\mathscr{U}}r_{5\kappa}\right] - \Omega^2\left[\overline{\mathscr{T}}r_{1\kappa} + \overline{\mathscr{T}}r_{2\kappa}\right] - \Omega\lambda\left[\overline{\mathscr{T}}r_{3\kappa}\right] - \lambda^2\left[\overline{\mathscr{T}}r_{4\kappa}\right]\right)\Bigg\}
\end{aligned} \tag{15}$$

where

$$\begin{aligned}
\overline{\mathscr{U}}r_{1\kappa} &= \overline{I}zr_\kappa\left\{\alpha(1+\xi\overline{e}r_\kappa - n^2\xi\overline{e}r_\kappa)\frac{\mathrm{d}\overline{w}}{\mathrm{d}\overline{x}} - n^2\xi\overline{u}\right\}^2,\\
\overline{\mathscr{U}}r_{2\kappa} &= \overline{I}xr_\kappa\left\{(1-n^2)\overline{w}\right\}^2,\\
\overline{\mathscr{U}}r_{3\kappa} &= \overline{A}r_\kappa\frac{(1+\xi\overline{e}r_\kappa)^2}{\xi}\left\{n\xi(1+\xi\overline{e}r_\kappa)\overline{v} + (1+n^2\xi\overline{e}r_\kappa)\overline{w}\right\}^2,\\
\overline{\mathscr{U}}r_{4\kappa} &= \overline{J}r_\kappa\frac{1}{2(1+\nu_\kappa)}\left\{-n\xi\overline{u} + \alpha n\frac{\mathrm{d}\overline{w}}{\mathrm{d}\overline{x}}\right\}^2,\\
\overline{\mathscr{U}}r_{5\kappa} &= \overline{A}r_\kappa\left\{\left(n\xi\overline{u} + \xi\overline{e}r_\kappa\alpha\frac{\mathrm{d}\overline{w}}{\mathrm{d}\overline{x}}\right)^2 + \left(n\xi(1+\xi\overline{e}r_\kappa)\overline{v} + (\xi\overline{e}r_\kappa n^2+1)\overline{w}\right)^2 + (\xi(1+\xi\overline{e}r_\kappa)\overline{v} + (\xi\overline{e}r_\kappa+1)n\overline{w})^2\right\},
\end{aligned} \tag{16}$$

and

$$\begin{aligned}
\overline{\mathscr{T}}r_{1\kappa} &= \overline{A}r_\kappa\left\{\left(\xi\overline{u} + \xi^2\overline{e}r_\kappa\alpha\frac{\mathrm{d}\overline{w}}{\mathrm{d}\overline{x}}\right)^2 + (\xi(1+\xi\overline{e}r_\kappa)\overline{v} + \xi\overline{e}r_\kappa n\overline{w})^2 + \overline{w}^2\right\},\\
\overline{\mathscr{T}}r_{2\kappa} &= \xi\alpha^2(\overline{I}xr_\kappa + \overline{I}zr_\kappa)\left(\frac{\mathrm{d}\overline{w}}{\mathrm{d}\overline{x}}\right)^2,\\
\overline{\mathscr{T}}r_{3\kappa} &= 4\overline{A}r_\kappa\left\{\xi(1+\xi\overline{e}r_\kappa)\overline{v}\overline{w} + \xi\overline{e}r_\kappa n\overline{w}^2\right\},\\
\overline{\mathscr{T}}r_{4\kappa} &= \overline{A}r_\kappa\left\{\xi^2(1+\xi\overline{e}r_\kappa)^2\overline{v}^2 + (n^2\xi^2\overline{e}r_\kappa^2+1)\overline{w}^2 + 2n\xi^2\overline{e}r_\kappa(1+\xi\overline{e}r_\kappa)\overline{v}\overline{w}\right\}.
\end{aligned} \tag{17}$$

2.3. Geometric boundary conditions

For simply supported cylindrical shells, four kinds of boundary conditions can be designated as follows:

$$S_1 : \overline{w} = \overline{v} = 0, \quad S_2 : \overline{w} = 0, \quad S_3 : \overline{w} = \overline{u} = 0, \quad S_4 : \overline{w} = \overline{v} = \overline{u} = 0. \tag{18}$$

2.4. Ritz functions

In view of satisfying the foregoing geometric boundary conditions, the proposed Ritz functions for approximating the displacements are:

$$\begin{aligned}
\overline{u} &= \left(\sum_{i=1}^{\mathrm{NS}} p_i\overline{x}^{i-1}\right)(\overline{x})^{P_u^0}(1-\overline{x})^{P_u^1} = \sum_{i=1}^{\mathrm{NS}} p_i\overline{u}_i,\\
\overline{v} &= \left(\sum_{i=1}^{\mathrm{NS}} q_i\overline{x}^{i-1}\right)(\overline{x})^{P_v^0}(1-\overline{x})^{P_v^1} = \sum_{i=1}^{\mathrm{NS}} q_i\overline{v}_i,\\
\overline{w} &= \left(\sum_{i=1}^{\mathrm{NS}} r_i\overline{x}^{i-1}\right)(\overline{x})^{P_w^0}(1-\overline{x})^{P_w^1} = \sum_{i=1}^{\mathrm{NS}} r_i\overline{w}_i,
\end{aligned} \tag{19}$$

where the powers of P are as shown in Table 1. The superscripts of P, i.e. 0 and 1, denote the cylindrical shell ends at $\overline{x} = 0$ and 1, respectively.

These forms of Ritz functions allow easy exact differentiation and integration. Also, by increasing the number of polynomials terms NS, better convergence to exact solution can be achieved.

Table 1
Powers of P for Ritz functions

Boundry condition	S_1	S_2	S_3	S_4
P_u	0	0	1	1
P_v	1	0	0	1
P_w	1	1	1	1

2.5. Equations of motion

Applying the Rayleigh–Ritz method (minimization of non-dimensional energy functional with respect to Ritz functions coefficients), the equations of motion are derived as follows:

$$\left.\begin{aligned}\frac{\partial \overline{F}}{\partial p_i} &= 0\\ \frac{\partial \overline{F}}{\partial q_i} &= 0\\ \frac{\partial \overline{F}}{\partial r_i} &= 0\end{aligned}\right\}, \quad i = 1, 2, \ldots, \mathrm{NS}. \tag{20}$$

Substituting Eq. (19) into Eq. (15) and then into Eq. (20) yields the following eigenvalue equation:

$$\left[[K] + \sum_{\kappa=1}^{N}[Kr_\kappa] + \lambda^2 \sum_{\kappa=1}^{N}[Kr_\kappa]_{\lambda^2} - \Omega^2\left([M] + \sum_{\kappa=1}^{N}[Mr_\kappa]\right) - \Omega\lambda\left([M]_\lambda + \sum_{\kappa=1}^{N}[Mr_\kappa]_\lambda\right) - \lambda^2\left([M]_{\lambda^2} + \sum_{\kappa=1}^{N}[Mr_\kappa]_{\lambda^2}\right)\right]\{C\} = \{0\}, \tag{21}$$

where $[K]$ and $[M]$ are stiffness and mass matrices of cylindrical shell, respectively. Also, $[Kr_\kappa]$ and $[Mr_\kappa]$ are corresponding matrices of the κth ring stiffener, $\{C\} = \{p_1, \ldots, p_{\mathrm{NS}}, q_1, \ldots, q_{\mathrm{NS}}, r_1, \ldots, r_{\mathrm{NS}}\}^{\mathrm{T}}$ is the column vector of Ritz coefficients, $\Omega^2 = (1-\nu^2)\rho R^2\omega^2/E$ is a non-dimensional frequency parameter, $\lambda^2 = (1-\nu^2)\rho R^2\varpi^2/E$ is a non-dimensional shell rotation speed parameter. Matrices with subscripts λ, λ^2 are the effect of stiffened shell rotation speed.

3. Results and discussions

3.1. Cylindrical shells with uniform ring spacing and eccentricity

Rayleigh–Ritz method (Eq. (21)) with proposed displacement functions (Eq. (19)) is used to determine the dynamic characteristics of two simply supported (S1–S1) ring stiffened cylindrical shells. The geometrical dimensions and material properties of these shells are given in Table 2. The M1 model is a non-rotating externally ring stiffened cylindrical shell with evenly spaced and uniform stiffeners eccentricity.

Table 3 shows the comparison between predicted analytical results of natural frequencies and the experimental results of Hoppmann [1] and the analytical results of Mustafa and Ali [6] for various modes of vibrations for M1 model. It could be observed that using polynomial terms of $\mathrm{NS} = 8$ for each displacement function is adequate for converged results. It should be noted that the results are in good agreement. Moreover, the agreements of the presented analytical results with the experimental values of Hoppmann are better than the analytical values of Mustafa and Ali. Therefore, applying this method with the proposed Ritz functions has adequate accuracy to determine the natural frequencies of ring stiffened cylindrical shells.

Table 2
Geometrical and material properties of two stiffened shells

Characteristics	Physical dimensions and values	
	M1 model	M2 model
Number of rings N	19	13
Shell radius R (m)	0.049759	0.203
Shell thickness h (m)	0.001651	0.00204
Shell length L (m)	0.3945	0.813
Ring depth dr, d_0 (m)	0.005334	0.006
Ring width br (m)	0.003175	0.004
Modulus of elasticity E (GPa)	68.95	207
Mass density ρ (kg/m^3)	2762	7430
Poisson's ratio v	0.3	0.3
Stiffening type	External	Internal (external)

Table 3
Convergence and comparison of natural frequencies with other references for model M1

Mode number		Present analysis results Natural frequencies (Hz)				Experimental [1]	Discrepancy[a] (%)	Analytical [6]
m	n	Number of polynomials: NS						
		4	6	8	10			
1	1	1199.85	1199.58	1199.58	1199.58	—	—	1204
	2	1564.52	1564.48	1564.48	1564.47	1530	2.2	1587
	3	4400.6	4388.49	4387.68	4387.59	4080	7.0	4462
	4	8405.96	8381.31	8378.1	8377.75	—	—	8559
	5	13556.7	13510.3	13500.4	13490.7	—	—	13780
2	1	3790.78	3499.62	3493.61	3493.59	—	—	3498
	2	2365.13	2118.1	2113.87	2113.84	2040	3.5	2129
	3	4444.75	4400.6	4400.59	4400.58	4090	7.0	4437
	4	8449.92	8393.05	8392.89	8392.63	—	—	8482
	5	13568.8	13566.7	13509.8	13508.9	—	—	13695
3	1	6543.24	5868.62	5840.25	5839.89	—	—	5844
	2	4111.98	3409.15	3378.59	3378.17	3200	5.2	3386
	3	4935.99	4607.88	4596.06	4595.79	4520	1.6	4627
	4	8496.7	8449.94	8449.93	8449.89	7520	11.0	8438
	5	13624.4	13624.3	13567.2	13555.4	—	—	13595

[a]Discrepancy between the presented analytical results and the experimental results [1].

3.2. Cylindrical shells with non-uniform ring spacing and eccentricity

Here, the effects of non-uniform rings spacing and non-uniform stiffeners eccentricity distribution are considered, separately and simultaneously. The main purpose of this study is to answer whether it is possible to obtain higher natural frequencies at non-uniform stiffeners distribution with constant stiffeners mass. To this end, M2 model with uniform stiffener distribution is considered, which its properties are shown in Table 2. Uniform distribution is the case of evenly spaced and equal depth for all stiffeners. Some cases of non-uniform rings spacing and non-uniform eccentricity distributions are shown in Fig. 2. The minimum depth of stiffeners is located at the two ends of the shell and the maximum depth of stiffeners is located at the midsection of the shell length. The maximum and minimum depth of stiffeners is determined, such that the mass and volume of stiffeners remain unchanged with respect to uniform distribution. Assuming the same width for all stiffeners,

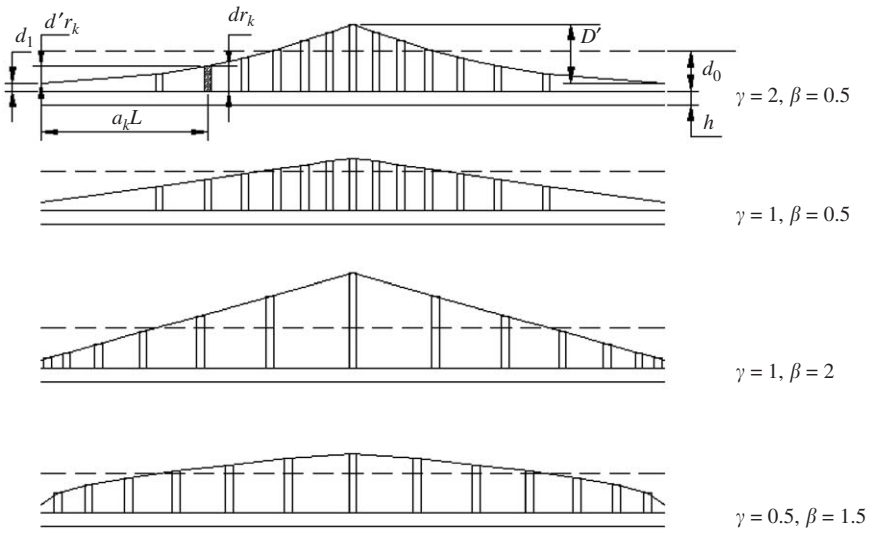

Fig. 2. Non-uniform rings spacing and non-uniform eccentricity distribution.

the volume of rings for externally stiffened shell can be written as:

$$V_{\text{uniform}} = 2\pi N\left(R + \frac{h + d_0}{2}\right) b d_0, \tag{22a}$$

$$V_{\text{non-uniform}} = 2\pi b\left(\sum_{\kappa=1}^{N}\left(R + d_1 + \frac{h + d'r_\kappa}{2}\right) d'r_\kappa\right) + 2\pi N\left(R + \frac{h + d_1}{2}\right) b d_1, \tag{22b}$$

where d_1 represents the minimum stiffeners depth and d_0 is the stiffeners depth in uniform distribution.

Equating the volume of stiffeners in uniform and non-uniform distributions, a second-order equation corresponding to D' can be obtained as follows:

$$\frac{1}{N}\left(\frac{D'}{R + d_1 + (h/2)}\right)^2 \sum_{\kappa=1}^{N} \psi' r_\kappa^2 + \frac{2}{N}\left(\frac{D'}{R + d_1 + (h/2)}\right) \sum_{\kappa=1}^{N} \psi' r_\kappa - \frac{2(R + (h/2))(d_0 - d_1)}{(R + d_1 + (h/2))^2} - \frac{(d_0^2 - d_1^2)}{(R + d_1 + (h/2))^2} = 0, \tag{23}$$

where D' denotes the difference between the maximum and minimum depth of non-uniformly stiffeners distribution.

For internally stiffened shell, the corresponding equation can be written as

$$-\frac{1}{N}\left(\frac{D'}{R - d_1 - (h/2)}\right)^2 \sum_{\kappa=1}^{N} \psi' r_\kappa^2 + \frac{2}{N}\left(\frac{D'}{R - d_1 - (h/2)}\right) \sum_{\kappa=1}^{N} \psi' r_\kappa - \frac{2(R - (h/2))(d_0 - d_1)}{(R - d_1 - (h/2))^2} + \frac{(d_0^2 - d_1^2)}{(R - d_1 - (h/2))^2} = 0. \tag{24}$$

Selecting a value for d_1, the value of D' can be determined by solving Eq. (23) or Eq. (24). The depth of each stiffener dr_κ would be obtained as follows:

$$\psi' r_\kappa = \frac{d'r_\kappa}{D'} = \begin{cases} (2a_\kappa)^\gamma & \kappa \leqslant N/2, \\ (2(1 - a_\kappa))^\gamma & \kappa > N/2, \end{cases} \tag{25}$$

$$a_\kappa = \left(\frac{k}{N+1}\right)^\beta, \quad \kappa = 1 \ldots N, \tag{26}$$

$$dr_\kappa = \psi' r_\kappa \times D' + d_1, \tag{27}$$

where in Fig. 2 and in Eqs. (25)–(27), γ and β represent the order of variations of eccentricity distribution function and rings spacing distribution function along the shell length, respectively.

For $\beta > 1$, the stiffeners concentration at the two ends of the shell is more than its middle. It means that the rings spacing in the middle section of the shell is greater than the rings spacing at the two ends. On the other hand, for $\beta < 1$, the ring stiffeners are compressed in the midsection of the shell length. In this study, β varies from 0.1 to 2. The $\beta = 1$ denotes the case of evenly spaced ring stiffeners along the shell length. Also, γ varies from 0 to 2. The case of $\gamma = 0$ and $\beta = 1$ denotes a uniform distribution of ring stiffeners along the shell length like the two models M1 and M2, as shown in Table 2.

Fig. 3(a–d) shows the variations of the natural frequencies of vibration with respect to depth ratio (d_1/d_0), corresponding to circumferential waves $n = 1$–5 and longitudinal wave $m = 1$, for different values of γ. Here, the rings spacing is uniform and only the effect of non-uniform eccentricity is considered.

It should be noted that, reduction of the depth ratio increases mass and stiffness in the middle section of the shell and decreases them at the two ends of the shell. Since the stiffness increase is more than the mass increase,

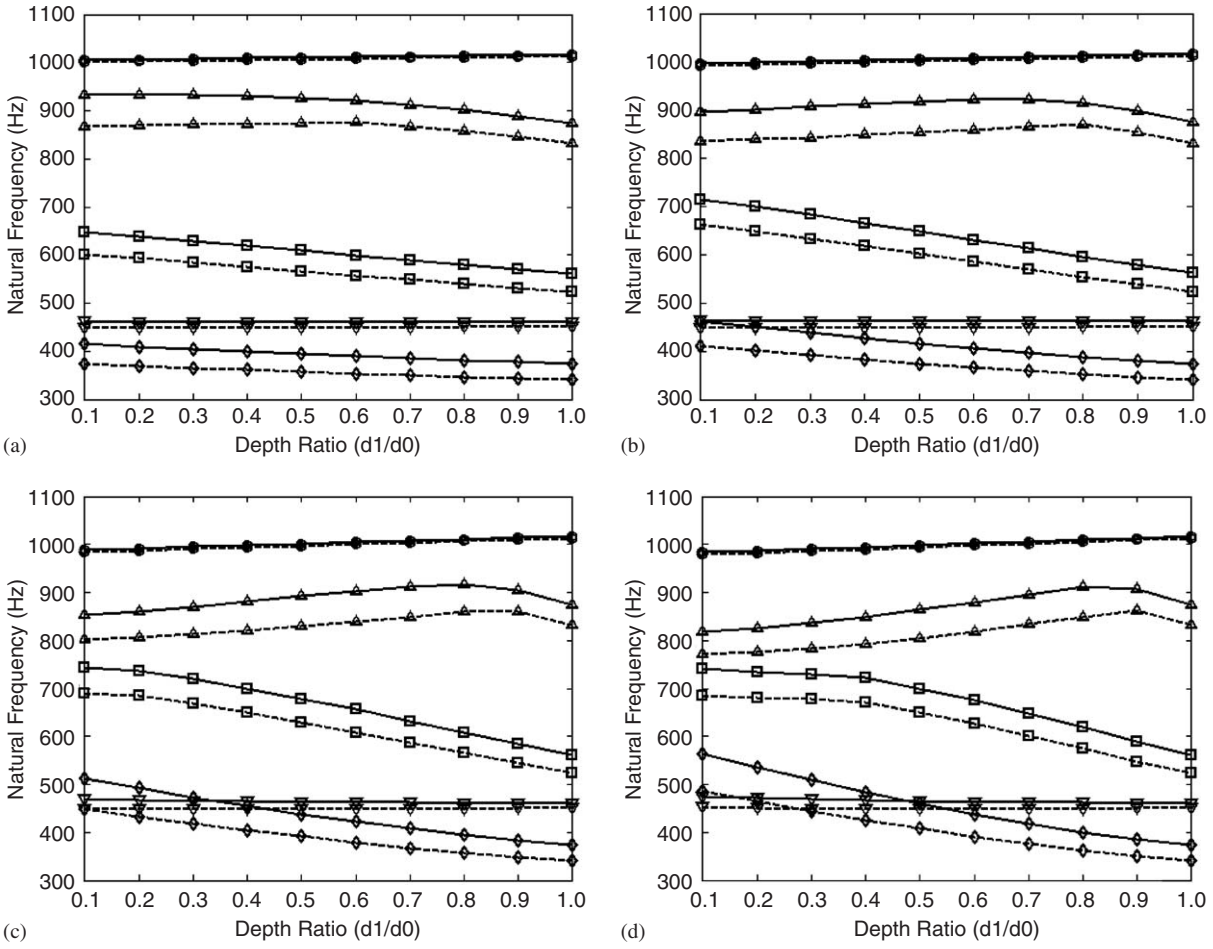

Fig. 3. Natural frequencies variations versus depth ratio for equal rings spacing ($\beta = 1$) and non-uniform eccentricity distribution: (a) $\gamma = 0.5$; (b) $\gamma = 1$; (c) $\gamma = 1.5$; (d) $\gamma = 2$, –○– $n = 1$, –▽– $n = 2$, –◇– $n = 3$, –□– $n = 4$, –△– $n = 5$, — internal ring, - - - external ring.

the natural frequencies of various circumferential modes (except beam mode frequency $n = 1$) increase. On the other hand, for higher depth ratios, a reduction in natural frequencies is observed for these modes.

Inversely, an increase of the depth ratio leads to higher beam mode frequency. In the beam mode, the shape of stiffeners remain circular and the strain energy of stiffeners dose not affect the total energy of the system and only the kinetic energy of stiffeners contributes in the total energy. Therefore, the increase of the depth ratio decrease the mass in the midsection of the shell, reduces the kinetic energy, and raises the beam mode natural frequency.

For $\gamma > 1$, some natural frequency curve crossing is observed for higher depth ratios. Moreover, the fundamental frequency mode switches from one to another mode, and a sudden reduction in the fundamental frequency is observed. This case occurs in Fig. 3(c,d) which the fundamental frequency mode switches from $n = 2$ to 3. In lower depth ratios, the fundamental frequency corresponds to $n = 2$. By increasing depth ratio, frequency curve crossing is occurred and the fundamental frequency mode switches to $n = 3$ and its value decreases suddenly. Therefore, at constant stiffeners mass, higher natural frequencies can be obtained by selecting lower values for d_1/d_0.

Moreover, internal stiffening is better than the external stiffening for increasing the natural frequencies of various modes of vibrations. Mathematically, the difference between sign of external and internal stiffening (Eq. (7)) affects the natural frequencies, significantly. Physically, at constant stiffeners mass, the eccentricity value and stiffness of internal rings is more than the external rings.

Fig. 4(a,b) shows fundamental frequency variations versus d_1/d_0, corresponding to different values of γ, for two types of internal and external stiffening. In this figure, stiffeners are evenly spaced along the shell length. The maximum fundamental frequency occurs at the smallest value of d_1/d_0. It should be mentioned that, for $\gamma > 1$, the fundamental frequency circumferential mode switches from one mode to another. This could be seen with an abrupt slope variation and a sudden reduction in frequency.

Fig. 5(a,b) shows fundamental frequency variations versus β, corresponding to different values of γ, for two types of internal and external stiffening. In this figure, d_1/d_0 is equal to 0.1 and the effects of non-uniform rings eccentricity distribution and non-uniform rings spacing distribution are considered simultaneously. In this case, the maximum fundamental frequency is obtained for $\gamma = 2$ and $\beta = 2$. This states that the best combination for increasing the fundamental frequency is to use a few thick rings at the midsection of the shell and to put the other rings at the two ends of the shell with more concentration at the two ends.

Fig. 6(a,b) shows these results for beam mode natural frequency variations. For beam mode, frequency variation is different from the aforementioned cases. As β increases, beam mode frequency rises and the maximum frequency is obtained at $\gamma = 0$ and $\beta = 2$.

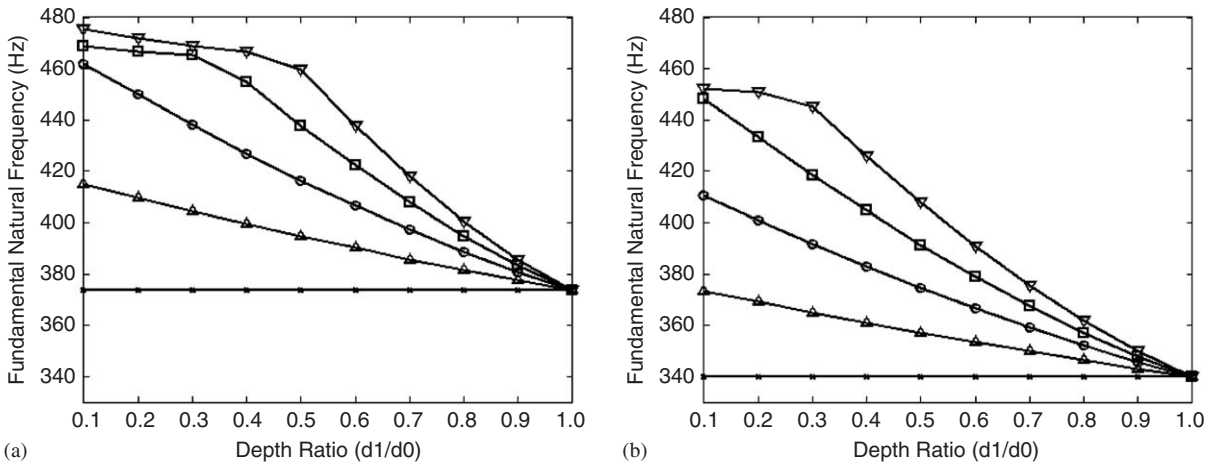

Fig. 4. Fundamental frequency variations versus depth ratio for non-uniform eccentricity distribution and equal rings spacing: (a) internal; (b) external, –▽– $\gamma = 2.0$, –□– $\gamma = 1.5$, –○– $\gamma = 1.0$, –△– $\gamma = 0.5$, —✖— $\gamma = 0.0$.

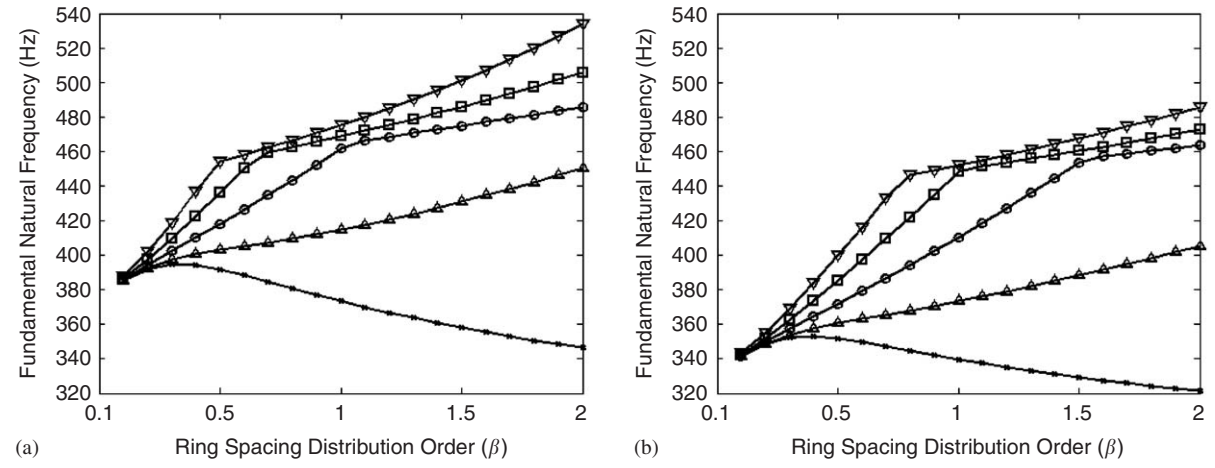

Fig. 5. Fundamental frequency variations versus β parameter corresponding different γ values: (a) internal; (b) external, $-\bigtriangledown-\ \gamma = 2.0$, $-\square-\ \gamma = 1.5$, $-\circ-\ \gamma = 1.0$, $-\triangle-\ \gamma = 0.5$, $\gamma = 0.0$.

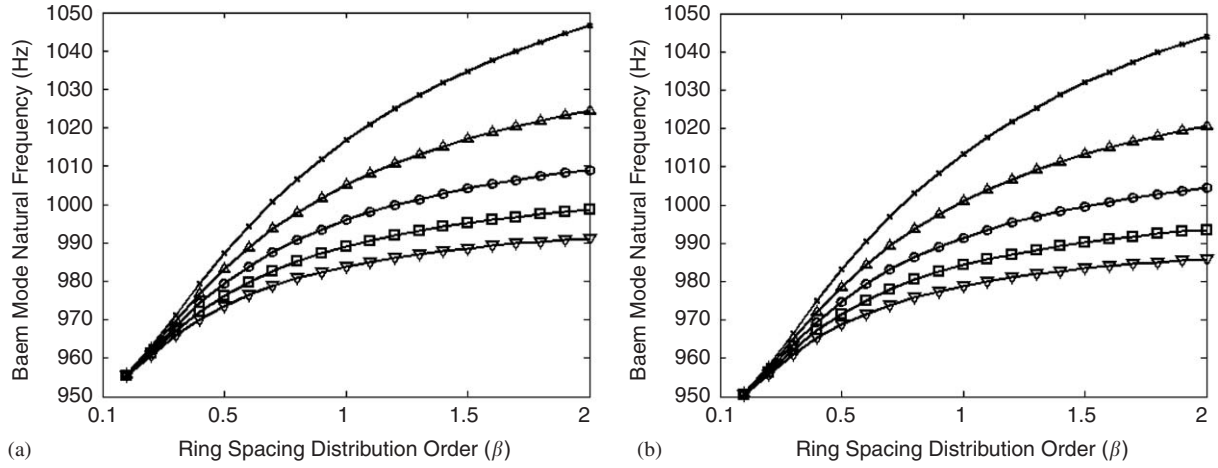

Fig. 6. Beam mode natural frequency variations versus β parameter corresponding different γ values: (a) internal; (b) external, $-\bigtriangledown-\ \gamma = 2.0$, $-\square-\ \gamma = 1.5$, $-\circ-\ \gamma = 1.0$, $-\triangle-\ \gamma = 0.5$, $\gamma = 0.0$.

It can be concluded that if the fundamental frequency occurs in the beam mode, selection of $\gamma = 0$ and $\beta = 2$ is the best combination to raise the frequency; otherwise, $\gamma = 2$ and $\beta = 2$ are preferred. Also, internal stiffening is better than the external stiffening to raise the fundamental frequency, as can be seen in these figures.

3.3. Rotating cylindrical shells with non-uniform ring spacing and eccentricity

At first, the effect of rotating speed on natural frequencies of un-stiffened cylindrical shells is considered. The comparison of the present results with the analytical results [16] is shown in Table 4. The agreements of results are good which the maximum observed discrepancy is less than 9%. It should be noted that the fundamental frequency occurs at $m = 1$ and $n = 5$.

Variations of fundamental frequency with the rotation speed (ϖ) of the internally ring stiffened cylindrical shell (M2 model), for different values of γ and β are shown in Fig. 7(a–d). It can be observed that, the frequencies split into two branches due to rotation. It should be noted that one branch (the lower) is, in fact,

Table 4
Comparison of frequency parameter for un-stiffened rotating cylindrical shell ($L/R = 5$, $h/R = 0.002$, $\nu = 0.3$, $\varpi = 10$ rad/s)

Mode number		Frequency parameter (Ω) Present analysis		Frequency parameter Ref. [16]		Discrepancy %	
m	n	Backward wave	Forward wave	Backward wave	Forward wave	Backward wave	Forward wave
1	1	0.1867	0.186	0.1864	0.185	0.16	0.53
	2	0.0762	0.0756	0.0773	0.0742	−1.44	1.85
	3	0.0384	0.038	0.0394	0.0374	−2.6	1.58
	4	0.0241	0.0237	0.0255	0.024	−5.8	−1.26
	5	0.0203	0.02	0.022	0.0215	−8.29	−7.5
	6	0.0241	0.0239	0.0262	0.0248	−8.71	−3.75
	7	0.0298	0.0294	0.0321	0.0316	−7.72	−7.48
	8	0.037	0.0368	0.0397	0.0394	−7.29	−7.06
2	1	0.4598	0.4591	0.4607	0.4605	−0.2	−0.3
	2	0.2407	0.2401	0.24	0.2397	0.29	0.16
	3	0.135	0.1346	0.1343	0.1341	0.52	0.37
	4	0.0839	0.0835	0.0834	0.0832	0.59	0.36
	5	0.0577	0.0574	0.058	0.0578	−0.52	−0.69
	6	0.0449	0.0447	0.0465	0.046	−3.5	−2.9
	7	0.0411	0.0409	0.0436	0.0434	−6	−6.11
	8	0.0437	0.0435	0.0464	0.0462	−6.17	−6.2

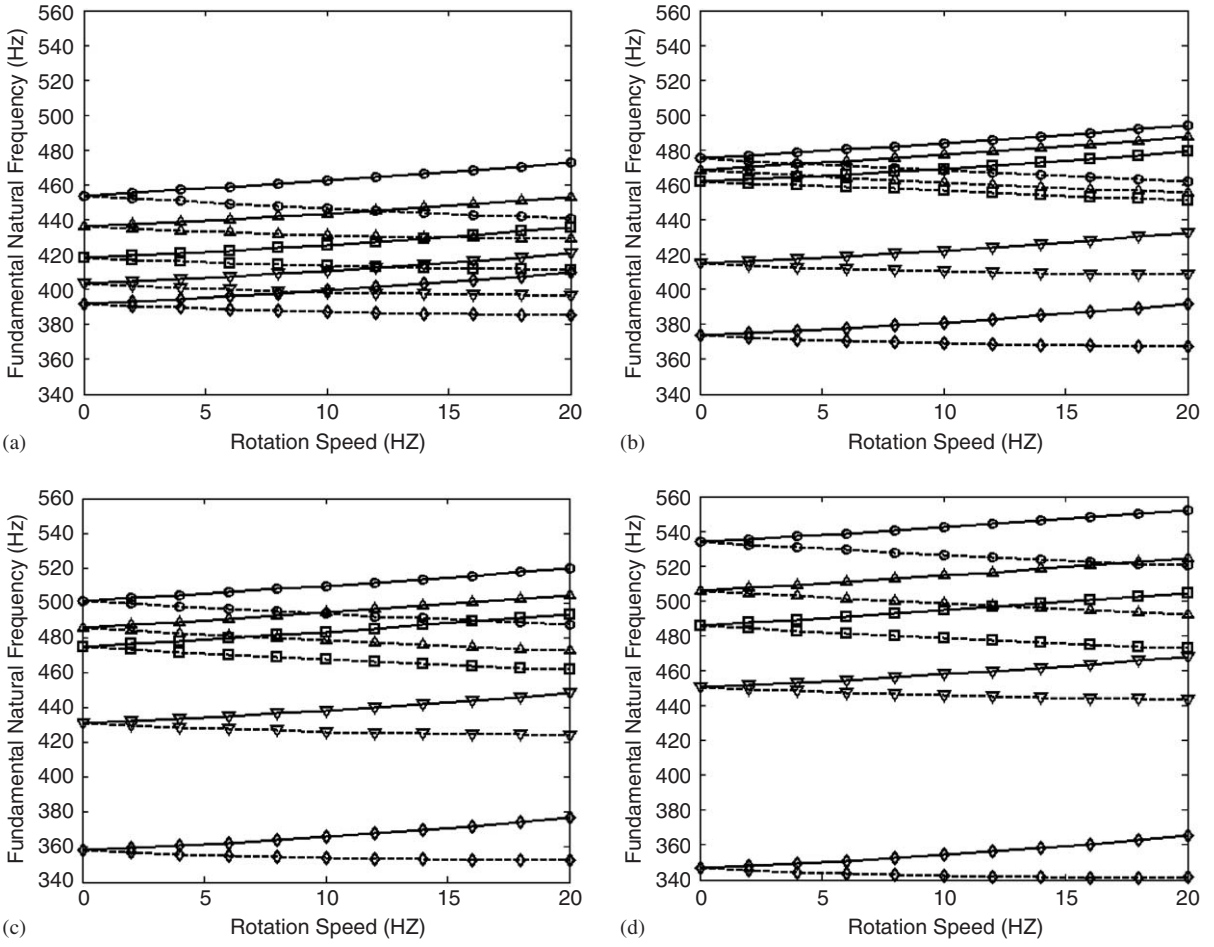

Fig. 7. Fundamental frequency variations versus rotation speed of internally ring stiffened shell for non-uniform eccentricity and non-uniform rings spacing: (a) $\beta = 0.5$; (b) $\beta = 1$; (c) $\beta = 1.5$; (d) $\beta = 2$, $-\bigcirc-$ $\gamma = 2.0$, $-\triangle-$ $\gamma = 1.5$, $-\square-$ $\gamma = 1.0$, $-\bigtriangledown-$ $\gamma = 0.5$, $-\diamond-$ $\gamma = 0.0$, — backward wave, - - - forward wave.

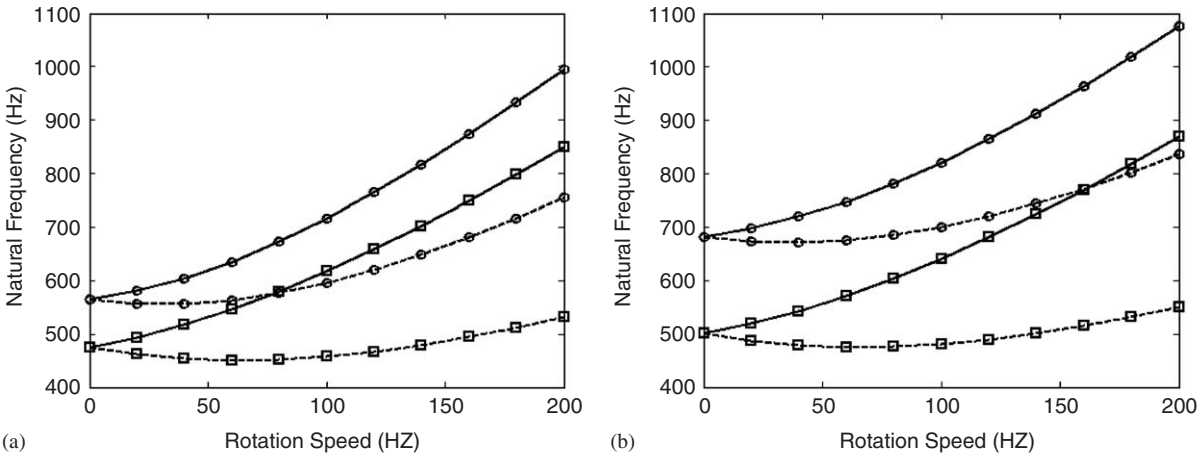

Fig. 8. Natural frequencies variations versus rotation speed of internally ring stiffened shell for non-uniform eccentricity and non-uniform rings spacing: (a) $\beta = 1$, $\gamma = 2$; (b) $\beta = 1.5$, $\gamma = 2$, $-\square- \; n = 2$, $-\circ- \; n = 3$, — backward wave, - - - forward wave.

comprised of negative frequencies based on Eq. (21). The figure shows only the absolute values. One of these two branches corresponds to the forward modes and other to the backward modes. Increase of the rotation speed raises the backward wave fundamental frequency in quadratic form for all values of γ and β. On the other hand, the forward wave fundamental frequency decrease with the increase of rotation speed. For the present shell model, the maximum fundamental frequency is obtained at γ and β values of 2.

Fig. 8(a,b) shows the variation of natural frequencies with the rotation speed of aforementioned stiffened cylindrical shell, for two cases of non-uniform stiffeners distribution corresponding to $m = 1$ and $n = 2, 3$. The bifurcation of natural frequencies due to rotation speed and Coriolis accelerations can be observed.

4. Conclusions

The free vibration analysis of the ring stiffened simply supported rotating cylindrical shells has been investigated via Ritz method by treating the stiffeners as discrete elements. The eigenvalue equation results have been validated by comparing with the results of the well-known natural frequency studies for non-rotating cylindrical shells with uniform ring stiffeners distribution. Some new natural frequency results for various orders of eccentricity distribution function and rings spacing distribution function have been presented. At constant stiffeners mass, various distributions of ring stiffeners results show that to increase the fundamental frequency, if this occur in beam mode, it is better to use $\gamma = 0$ and $\beta = 2$; otherwise, it is better to use $\gamma = 2$ and $\beta = 2$. Moreover, the non-uniform stiffeners distribution significantly affects the dynamic characteristics of stiffened shell. Some natural frequency curves crossing with each other and sudden decrement in fundamental frequency can be explained by the effects of stiffeners distribution. Also, internal stiffening is better than the external stiffening to raise the natural frequencies. Moreover, the effect of rotating speed on fundamental frequency of internally ring stiffened cylindrical shells for various distributions has been investigated. The results show that an increase in the rotation speed of the shell leads to an increase in natural frequencies in quadratic form. Furthermore, bifurcation of natural frequencies due to rotation speed and Coriolis acceleration is investigated.

At constant stiffeners mass, selection of the best distribution parameters values can increase natural frequencies significantly. Therefore, it is important to study the optimal distribution of ring stiffeners for further enhancement of natural frequencies.

References

[1] W.H. Hoppmann, Some characteristics of the flexural vibrations of orthogonally stiffened cylindrical shells, *Journal of Acoustical Society of America* 30 (1958) 77–82.

[2] M.M. Mikulas Jr., J.A. McElman, On the free vibration of eccentrically stiffened cylindrical shells and plates, NASA TN-D 3010 1965.
[3] D.M. Egle, J.L. Sewall, Analysis of free vibration of orthogonally stiffened cylindrical shells with stiffeners treated as discrete elements, *AIAA Journal* 6 (3) (1968) 518–526.
[4] S. Parthan, D.J. Johns, Effects of in-plane and rotary inertia on the frequencies of eccentrically stiffened cylindrical shells, *AIAA Journal* 8 (1970) 253–261.
[5] A. Rosen, J. Singer, Vibrations of axially loaded stiffened cylindrical shells, *Journal of Sound and Vibration* 34 (3) (1974) 357–378.
[6] B.A.J. Mustafa, R. Ali, An energy method for free vibration analysis of stiffened circular cylindrical shells, *Computer & Structures* 32 (2) (1989) 335–363.
[7] C.W. Lim, K.M. Liew, A pb-2 Ritz formulation for flexural vibration of shallow cylindrical shells of rectangular planform, *Journal of Sound and Vibration* 173 (3) (1994) 343–375.
[8] K.M. Liew, C.W. Lim, A global continuum Ritz formulation for flexural vibration of pretwisted trapezoidal plates with one edge built in, *Computer Methods in Applied Mechanics and Engineering* 114 (1994) 233–247.
[9] K.M. Liew, C.W. Lim, Vibratory characteristics of cantilevered rectangular shallow shells of variable thickness, *AIAA Journal* 32 (2) (1994) 387–396.
[10] S. Swaddiwudhipong, J. Tian, C.M. Wang, Vibrations of cylindrical shells with intermediate supports, *Journal of Sound and Vibration* 187 (1) (1995) 69–93.
[11] C.M. Wang, S. Swaddiwudhipong, J. Tian, Ritz method for vibration analysis of cylindrical shells with ring stiffeners, *Journal of Engineering Mechanics* 123 (1997) 134–142.
[12] G.H. Bryan, On the beats in the vibration of a revolving cylinder or bell, *Proceedings of the Cambridge Philosophical Society* 7 (1890) 101–111.
[13] R.A. DiTaranto, M. Lessen, Coriolis acceleration effect on the vibration of a rotating thin walled circular cylinder, *ASME Journal of Applied Mechanics* 31 (1964) 700–701.
[14] S.C. Huang, W. Soedel, Effects of coriolis acceleration on the forced vibration of rotating cylindrical shells, *ASME Journal of Applied Mechanics* 55 (1988) 231–233.
[15] X. Zhao, K.M. Liew, T.Y. Ng, Vibration of rotating cross-ply laminated circular cylindrical shells with stringer and ring stiffeners, *International Journal of Solids and Structures* 39 (2002) 529–545.
[16] K.M. Liew, T.Y. Ng, X. Zhao, J.N. Reddy, Harmonic reproducing kernel particle method for free vibration analysis of rotating cylindrical shells, *Computer Methods in Applied Mechanics and Engineering* 191 (2002) 4141–4157.
[17] J.L. Sanders, An improved first-approximation theory for thin shells, NASA TR R-24 1959.